

Measurement of D_s^\pm and D^\pm Decays to Nonstrange States

J. C. Anjos,⁽³⁾ J. A. Appel,⁽⁵⁾ A. Bean,⁽¹⁾ S. B. Bracker,⁽⁸⁾ T. E. Browder,⁽¹⁾ L. M. Cremaldi,^{(4),(a)} J. R. Elliott,^{(4),(b)} C. O. Escobar,⁽⁷⁾ P. Estabrooks,⁽²⁾ M. C. Gibney,⁽⁴⁾ G. F. Hartner,⁽⁸⁾ P. E. Karchin,⁽⁹⁾ B. R. Kumar,⁽⁸⁾ M. J. Losty,⁽⁶⁾ G. J. Luste,⁽⁸⁾ P. M. Mantsch,⁽⁵⁾ J. F. Martin,⁽⁸⁾ S. McHugh,⁽¹⁾ S. R. Menary,⁽⁸⁾ R. J. Morrison,⁽¹⁾ T. Nash,⁽⁵⁾ P. Ong,⁽⁸⁾ J. Pinfold,⁽²⁾ G. Punkar,⁽¹⁾ M. V. Purohit,^{(5),(c)} J. R. Raab,^{(1),(d)} A. F. S. Santoro,⁽³⁾ J. S. Sidhu,^{(2),(e)} K. Sliwa,⁽⁵⁾ M. D. Sokoloff,^{(5),(f)} M. H. G. Souza,⁽³⁾ W. J. Spalding,⁽⁵⁾ M. E. Streetman,⁽⁵⁾ A. B. Stundžia,⁽⁸⁾ and M. S. Witherell⁽¹⁾

⁽¹⁾University of California, Santa Barbara, California 93106

⁽²⁾Carleton University, Ottawa, Ontario, Canada K1S5B6

⁽³⁾Centro Brasileiro de Pesquisas Fisicas, Rio de Janeiro, Brazil

⁽⁴⁾University of Colorado, Boulder, Colorado 80309

⁽⁵⁾Fermi National Accelerator Laboratory, Batavia, Illinois 60510

⁽⁶⁾National Research Council, Ottawa, Ontario, Canada K1A0R6

⁽⁷⁾Universidade de São Paulo, 01000 São Paulo, Brazil

⁽⁸⁾University of Toronto, Toronto, Ontario, Canada M5S1A7

⁽⁹⁾Yale University, New Haven, Connecticut 06511

(Received 25 July 1988)

Using the data from Fermilab experiment 691, we have observed signals for the decays D_s^\pm and $D^\pm \rightarrow \pi^- \pi^+ \pi^\pm$ and have analyzed these modes for the fraction due to $\rho^0 \pi^\pm$ and $f_0(975) \pi^\pm$. In addition, we have searched for the decays D_s^\pm and $D^\pm \rightarrow \pi^- \pi^+ \pi^- \pi^+ \pi^\pm$. Values or upper limits are reported for the relative branching fractions for all of the above decays.

PACS numbers: 13.25.+m, 14.40.Jz

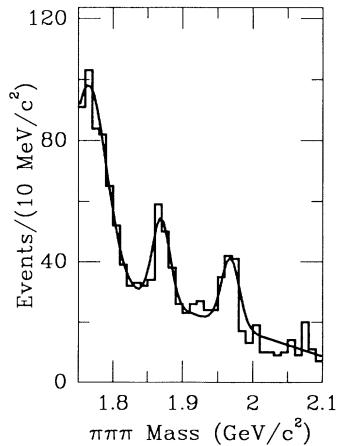
A notable feature of the charmed mesons is the difference in their lifetimes¹: The D^+ lifetime is more than twice that of the D^0 or D_s^+ . Among the possible explanations are that (1) nonspectator diagrams, not available in D^+ decay, have amplitudes comparable to those of spectator diagrams for the D^0 and D_s^+ , and (2) the D^+ decay rate is suppressed by destructive interference of spectator diagrams, which cannot occur for the D^0 and D_s^+ . Although previous measurements of a number of charm-decay modes bear on these explanations,² we consider here two relatively unexplored decays. A consequence of explanation (1) might be an observable rate for the decay $D_s^\pm \rightarrow \pi^- \pi^+ \pi^\pm$, which could occur via the Cabibbo-allowed annihilation subprocess $c\bar{s} \rightarrow W^+ \rightarrow u\bar{d}$, but is unlikely to occur via the spectator diagram. The explanation (2) suggests that the decay rate for $D^\pm \rightarrow \pi^- \pi^+ \pi^\pm$ could be suppressed relative to that for $D^\pm \rightarrow K^- K^+ \pi^\pm$ since interference is possible for the former decay but not the latter.

In this paper, we report the first observation of the decay $D_s^\pm \rightarrow \pi^- \pi^+ \pi^\pm$ and the most accurate measurement to date of the decay $D^\pm \rightarrow \pi^- \pi^+ \pi^\pm$. For both of these decays, we determine the fraction of $\pi^- \pi^+ \pi^\pm$ decays due to the quasi-two-body states $\rho^0 \pi^\pm$ and $f_0 \pi^\pm$. We also report on the results of a search for D_s^\pm and $D^\pm \rightarrow \pi^- \pi^+ \pi^- \pi^+ \pi^\pm$. Henceforth, each decay mode will stand implicitly for the charge-conjugate mode as well.

This study utilizes the sample of 10^8 events recorded from Fermilab experiment 691,¹ in which high-energy

photon-beryllium interactions were detected with a silicon vertex hodoscope, magnetic spectrometer, and multicell threshold Cherenkov counters. To reduce the computing load for detailed event analysis, a data subset was extracted by performing a general vertex reconstruction, producing a list of possible vertices with $\chi^2/N_{DF} < 3$, and then selecting events with secondary vertices. Events with a three-prong charm-decay candidate are required to have the following vertex properties: There is at least one downstream vertex that has three and only three tracks, the secondary vertex does not share tracks with any vertex candidate upstream of it, all three tracks go through both magnets, and the summed three-momentum vector of the secondary tracks points back to the primary vertex with an impact parameter less than $80 \mu\text{m}$. In addition, the vertex separation Δz along the beam direction is greater than $15\sigma_{\Delta z}$, where $\sigma_{\Delta z}$ is the error in Δz . The cut of $15\sigma_{\Delta z}$ is more stringent than that used in our previous analysis³ of $D_s^+ \rightarrow K^- K^+ \pi^+$ where the combination of Cherenkov identification of a kaon and vertex cut in the range $(6-10)\sigma_{\Delta z}$ provided sufficient background reduction. In our analysis for D_s^+ and $D^+ \rightarrow \pi^- \pi^+ \pi^+$ the tracks from the secondary vertex are required to have Cherenkov-counter pulse heights consistent with the $\pi\pi\pi$ mass hypothesis.

A $\pi^- \pi^+ \pi^+$ mass plot, with the cuts described above, is shown in Fig. 1. There are clear peaks for both the D^+ and the D_s^+ . The peak at $1.75 \text{ GeV}/c^2$ is due to the decays $D^+ \rightarrow K^- \pi^+ \pi^+$ which are misidentified as $\pi^- \pi^+ \pi^+$. A maximum-likelihood fit, shown in the fig-

FIG. 1. Histogram of $\pi^- \pi^+ \pi^+$ mass combinations.

ure, gives $82.6 \pm 15.3 D^+$ decays and $68.1 \pm 12.4 D_s^+$ decays. The fit is with Gaussian signals and a background shape that is the sum of a linear term and a Gaussian term for the false peak. The masses are fixed at $1.869 \text{ GeV}/c^2$ for the D^+ and $1.968 \text{ GeV}/c^2$ for the D_s^+ , and the widths are fixed on the basis of a Monte Carlo analysis, as are the parameters for the shape of the false peak.

To demonstrate the resonant structure of these decays, Dalitz plots are shown in Fig. 2(a) for the mass range 1.854 to $1.884 \text{ GeV}/c^2$, encompassing the D^+ , and in 2(b) for the range 1.953 to $1.983 \text{ GeV}/c^2$, encompassing the D_s^+ . In these Dalitz plots, the $\pi^- \pi^+$ combination with the higher invariant mass is plotted on the vertical axis. To determine if any $\pi^- \pi^+$ resonances are present, projections of a given Dalitz plot are made onto both the vertical and horizontal axes and then summed to give a histogram containing two entries of $\pi^- \pi^+$ invariant mass for each $\pi^- \pi^+ \pi^+$ event. These histograms are shown in Fig. 3. There is evidence for $D^+ \rightarrow \rho^0 \pi^+$ in histogram 3(a) and $D_s^+ \rightarrow f_0(975) \pi^+$ in 3(b). The $f_0(975)$, formerly called the S^* , is an $s\bar{s}$ resonance below $K\bar{K}$ threshold which decays primarily to pions.

To determine the fraction of $\pi^- \pi^+ \pi^+$ decays due to $\rho \pi^+$ or $f_0 \pi^+$, a maximum-likelihood fit is made to the distribution of $\pi^- \pi^+ \pi^+$ decay candidates taking into account, for each decay, the $\pi^- \pi^+$ invariant mass and the two $\pi^- \pi^+$ invariant-mass combinations. The $\pi^- \pi^+ \pi^+$ invariant mass is restricted to the range 1.820 to $1.920 \text{ GeV}/c^2$ for the D^+ fit, and the range 1.920 to $2.020 \text{ GeV}/c^2$ for the D_s^+ fit. The assumed probability density p is of the form

$$p(\pi^- \pi_1^+ \pi_2^+) = \sum_{i=1}^4 F_i(\pi^- \pi^+ \pi^+) f_i(\pi^- \pi_1^+, \pi^- \pi_2^+) c_i N_i, \quad (1)$$

where the terms i are due to (1) nonresonant (NR)

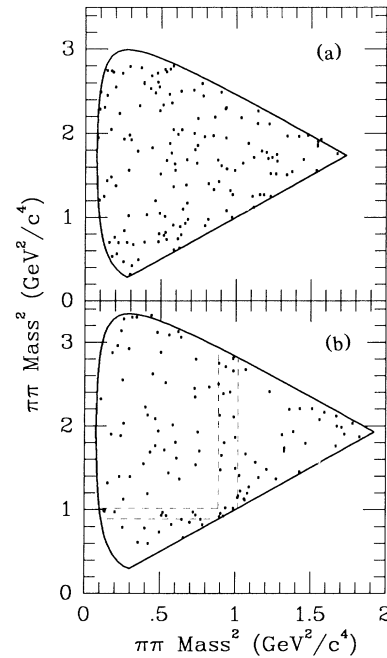


FIG. 2. Dalitz plot of $(\pi^- \pi_1^+ \text{ mass})^2$ versus $(\pi^- \pi_2^+ \text{ mass})^2$ for (a) events with $\pi^- \pi_1^+ \pi_2^+$ mass in the range 1.854 – $1.884 \text{ GeV}/c^2$, and (b) events with $\pi^- \pi_1^+ \pi_2^+$ mass in the range 1.953 – $1.983 \text{ GeV}/c^2$. The dotted lines in (b) bound the region within $\pm \Gamma$ (Breit-Wigner width) of the f_0 mass.

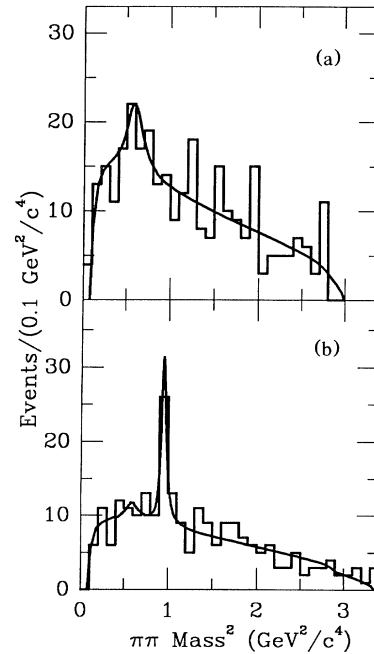


FIG. 3. Sum of Dalitz-plot projections onto $(\pi^- \pi_1^+ \text{ mass})^2$ axis and $(\pi^- \pi_2^+ \text{ mass})^2$ axis; (a) and (b) of this figure correspond to (a) and (b) of Fig. 2.

three-body decay, (2) quasi-two-body decay, (3) $\pi^- \pi^+ \pi^+$ combinatoric background, and (4) background from $\rho^0 \rightarrow \pi^- \pi^+$ in combination with an unrelated π^+ . The functions F_i give the dependence on the $\pi^- \pi^+ \pi^+$ invariant mass, previously discussed, and the functions f_i give the form of the distribution over the Dalitz plot. The nonresonant background is constant over the Dalitz plot and symmetric under interchange of the two identical π^+ mesons. For the decay $D^+ \rightarrow \rho^0 \pi^+$, $f = |a_\rho(\pi^- \pi_1^+) + a_\rho(\pi^- \pi_2^+)|^2$, where

$$a_\rho(\pi^- \pi_1^+) = \frac{\Gamma_\rho/2}{m(\pi^- \pi_1^+) - m(\rho) + i\Gamma_\rho/2} \cos(\theta_{\pi^- \pi_2^+}).$$

Note that f properly describes the nontrivial interference between the $\pi^- \pi_1^+$ and $\pi^- \pi_2^+$ amplitudes. For the decay $D_s^+ \rightarrow f_0 \pi^+$, $f = |a_f(\pi^- \pi_1^+) + a_f(\pi^- \pi_2^+)|^2$, where the amplitude a_f has the form⁴ of a coupled-channel Breit-Wigner resonance with parameters fixed from data⁴ for $\Psi \rightarrow f_0 + X$. The amplitude a_f does not depend on $\cos(\theta)$ since the f_0 has spin 0. The $\pi^- \pi^+ \pi^+$ combinatoric background was found to be uniformly distributed over the Dalitz plot. For the $\rho^0 \pi^+$ background, $f = |a(\pi^- \pi_1^+)|^2 + |a(\pi^- \pi_2^+)|^2$, where a is the Breit-Wigner amplitude for the ρ with no dependence on $\cos(\theta)$. The constants c_i provide the normalization for the functions f_i in Eq. (1). Each c_i is the reciprocal of the integral of f_i over the Dalitz plot for a given $\pi^- \pi^+ \pi^+$ mass. The parameters N_i are determined from the fit and give the number of events of each type i . The fitting procedure described above gives $N(D_s^+ \rightarrow f_0 \pi^+) = 22.4 \pm 7.3$ and $N(D^+ \rightarrow \rho^0 \pi^+) = 19.1 \pm 11.3$. The fits are superimposed on the projections of Dalitz plots in Fig. 3.

When interference between the $\rho^0 \pi^+$ and s -wave $\pi^- \pi^+ \pi^+$ signal amplitudes was allowed in the fit, no significant change was found in the fitted number of these decays for either the D^+ or the D_s^+ . When terms were included in the fit to allow for $D^+ \rightarrow f_0 \pi^+$ and $D_s^+ \rightarrow \rho^0 \pi^+$, no significant signals were found for these

modes. For $D_s^+ \rightarrow \rho^0 \pi^+$, the fit gave -1.7 ± 7.7 events.

To compute relative branching fractions for D_s^+ and D^+ decays, we chose to normalize to the most easily measured decay modes: $D_s^+ \rightarrow \phi \pi^+$ and $D^+ \rightarrow K^- \pi^+ \pi^+$. To obtain signals for these decays, we used tracking and vertex requirements identical to those used for the 3π decays. Cherenkov cuts were chosen appropriately for $D^+ \rightarrow K^- \pi^+ \pi^+$, but no Cherenkov cuts were used for the decay $D_s^+ \rightarrow \phi \pi^+$, $\phi \rightarrow K^- K^+$. For the latter decay, the $K^- K^+$ mass was required to be in the range 1.012 to 1.027 GeV/ c^2 , and it was required that $|\cos(\theta_{K\pi})| > 0.3$. These cuts yielded signals of 77.5 ± 9.4 $D_s^+ \rightarrow \phi \pi^+$ events and 2214 ± 62 $D^+ \rightarrow K^- \pi^+ \pi^+$ events. Mass plots for these decays, from the E691 data and with cuts similar to those used here, have been previously published.¹

The relative branching ratios B of three-body states reported in this paper are nearly independent of the properties of our apparatus because these ratios compare decays of identical particles to final states that differ only by the particle masses, m_π or m_K . A Monte Carlo simulation was used to determine that the ratios of acceptances, A , are $A(D_s^+ \rightarrow \pi^- \pi^+ \pi^+)/A(D_s^+ \rightarrow K^- K^+ \pi^+, K^- K^+ \text{ from } \phi) = 1.00 \pm 0.10$, and $A(D^+ \rightarrow \pi^- \pi^+ \pi^+)/A(D^+ \rightarrow K^- \pi^+ \pi^+) = 1.06 \pm 0.08$. For both D_s^+ and $D^+ \rightarrow \pi^- \pi^+ \pi^+$, the acceptance over the Dalitz plot was found to be uniform. Our results for relative branching ratios B are shown in Table I.

There is no significant contribution to the decay $D_s^+ \rightarrow \pi^- \pi^+ \pi^+$ from $\rho^0 \pi^+$. Our upper limit for the decay $D_s^+ \rightarrow \rho^0 \pi^+$ is nearly 3 times smaller than the existing limit.⁵ To determine the rate for $D_s^+ \rightarrow \pi^- \pi^+ \pi^+$ due to annihilation, we exclude the contribution from the decay $D_s^+ \rightarrow f_0 \pi^+$ which most likely originates from the $s\bar{s}$ quark pair present after spectator-diagram decay and not from annihilation. Thus, the nonzero rate for $D_s^+ \rightarrow (\pi^- \pi^+ \pi^+)_{\text{NR}}$ (given in Table I) is a measure of annihilation, and can be compared to the rate due to the spectator-diagram decay $D_s^+ \rightarrow K^- K^+ \pi^+$ by combining the results presented here with previously published data

TABLE I. Relative branching ratios (B) for D_s^+ and $D^+ \rightarrow$ nonstrange states. Errors are given in the following form: \pm statistical \pm systematic.

| Decay mode 1 | Decay mode 2 | $\frac{B(\text{decay mode 1})}{B(\text{decay mode 2})}$ |
|---|-----------------------------------|---|
| $D_s^+ \rightarrow \pi^- \pi^+ \pi^+$ | $D_s^+ \rightarrow \phi \pi^+$ | $0.44 \pm 0.10 \pm 0.04$ |
| $D_s^+ \rightarrow (\pi^- \pi^+ \pi^+)_{\text{NR}}$ | $D_s^+ \rightarrow \phi \pi^+$ | $0.29 \pm 0.09 \pm 0.03$ |
| $D_s^+ \rightarrow \rho^0 \pi^+$ | $D_s^+ \rightarrow \phi \pi^+$ | < 0.08 (90% C.L.) |
| $D_s^+ \rightarrow f_0 \pi^+$ | $D_s^+ \rightarrow \phi \pi^+$ | $0.28 \pm 0.10 \pm 0.03$ |
| $D^+ \rightarrow \pi^- \pi^+ \pi^+$ | $D^+ \rightarrow K^- \pi^+ \pi^+$ | $0.035 \pm 0.007 \pm 0.003$ |
| $D^+ \rightarrow (\pi^- \pi^+ \pi^+)_{\text{NR}}$ | $D^+ \rightarrow K^- \pi^+ \pi^+$ | $0.027 \pm 0.007 \pm 0.002$ |
| $D^+ \rightarrow \rho^0 \pi^+$ | $D^+ \rightarrow K^- \pi^+ \pi^+$ | < 0.015 (90% C.L.) |
| $D_s^+ \rightarrow \pi^- \pi^+ \pi^- \pi^+ \pi^+$ | $D_s^+ \rightarrow \phi \pi^+$ | < 0.29 (90% C.L.) |
| $D^+ \rightarrow \pi^- \pi^+ \pi^- \pi^+ \pi^+$ | $D^+ \rightarrow K^- \pi^+ \pi^+$ | < 0.019 (90% C.L.) |

from this experiment.⁶ We find

$$\frac{B(D_s^+ \rightarrow \pi^- \pi^+ \pi^+)_{\text{NR}}}{B(D_s^+ \rightarrow K^- K^+ \pi^+)} = 0.14 \pm 0.04.$$

Thus, the rate for D_s^+ decay that can be attributed to annihilation is small compared to that due to the spectator diagram. This suggests that annihilation is not the dominant cause of the $D_s^+ - D^+$ lifetime difference.

It might be possible that the annihilation contribution to the total D_s^+ decay rate is dominated by high-multiplicity modes. To test this hypothesis, and to search for new decay modes, we performed an analysis for the decays D^+ and $D_s^+ \rightarrow \pi^- \pi^+ \pi^- \pi^+ \pi^+$ using techniques similar to those described for D^+ and $D_s^+ \rightarrow \pi^- \pi^+ \pi^+$. No signals for the 5π modes were apparent. A maximum-likelihood fit to the 5π mass plot gave event estimates that were used to establish the 90%-confidence-level (C.L.) limits shown in Table I.

Our result, $B(D^+ \rightarrow \pi^- \pi^+ \pi^+)/B(D^+ \rightarrow K^- \pi^+ \pi^+) = 0.035 \pm 0.007 \pm 0.003$, is consistent with the Mark III value⁷ $0.042 \pm 0.16 \pm 0.010$. Using the results given here and previous data from E691, we find

$$\frac{B(D^+ \rightarrow \rho^0 \pi^+) P(\phi\pi)}{B(D^+ \rightarrow \phi \pi^+) P(\rho\pi)} < 0.16 \quad (90\% \text{ C.L.})$$

and

$$\frac{B(D^+ \rightarrow \pi^- \pi^+ \pi^+)_{\text{NR}} P(KK\pi)}{B(D^+ \rightarrow K^- K^+ \pi^+)_{\text{NR}} P(\pi\pi\pi)} = 0.18 \pm 0.06,$$

where P is the phase-space factor. Thus, decay modes in which destructive interference is possible are clearly suppressed relative to those without interference.

In conclusion, we have measured a nonzero-decay rate for $D_s^+ \rightarrow \pi^- \pi^+ \pi^+$ and have determined that the par-

tial rate which can be attributed to annihilation does not have a large effect on the $D_s^+ - D^+$ lifetime difference. Our measurement of the decay rate for $D^+ \rightarrow \pi^- \pi^+ \pi^+$ strengthens the existing evidence for suppression relative to the rate for $D^+ \rightarrow K^- K^+ \pi^+$, an effect which can be interpreted as evidence for the destructive interference of spectator diagrams.

This research was supported by the U.S. Department of Energy, the Natural Science and Engineering Council of Canada through the Institute of Particle Physics, the National Research Council of Canada, and the Brazilian Conselho Nacional de Desenvolvimento Científico e Tecnológico.

^(a)Now at the University of Mississippi, University, MS 38677.

^(b)Now at Electromagnetic Applications, Inc., Denver, CO 80201.

^(c)Now at Princeton University, Princeton, NJ 08544.

^(d)Now at EP Division, CERN, CH-1211 Geneva, Switzerland.

^(e)Deceased.

^(f)Now at the University of Cincinnati, Cincinnati, OH 45221.

¹J. R. Raab *et al.*, Phys. Rev. D **37**, 2391 (1988).

²I. I. Bigi, in *International Symposium on Production and Decay of Heavy Flavors*, edited by E. Bloom and A. Fridman [Ann. N.Y. Acad. Sci. **535**, 333 (1988)].

³J. C. Anjos *et al.*, Phys. Rev. Lett. **58**, 18 (1987).

⁴G. Gidal *et al.*, Phys. Lett. **107B**, 153 (1981).

⁵H. Albrecht *et al.*, Phys. Lett. **B 195**, 102 (1987).

⁶J. C. Anjos *et al.*, Phys. Rev. Lett. **60**, 897 (1988).

⁷R. M. Baltrusaitis *et al.*, Phys. Rev. Lett. **55**, 150 (1985); R. M. Baltrusaitis *et al.*, Phys. Rev. Lett. **56**, 2140 (1986).